A Helical Poly(amino acid) Having Carbazole Side Chains: A Candidate for a Photoelectric Liquid Crystal. 2. Steady-State and Time-Resolved Studies of Excimer Emission

Derek Biddle*

Institute of Physical Chemistry, University of Gothenburg and Chalmers University of Technology, S-412 96 Gothenburg, Sweden

L. Lawrence Chapoy

Instituttet for Kemiindustri, The Technical University of Denmark, 2800 Lyngby, Denmark.
Received April 13, 1983

ABSTRACT: The excimer emission from poly[N^{ϵ}-(-9-carbazolyl)carbonyl-L-lysine] (PKL) has been studied by steady-state and time-resolved techniques. Two well-resolved emission bands are observed, each showing slight structure. Time-resolved studies show that the low-energy band is due to two excimer species that are formed from excited species emitting in the high-energy band. Both of these may be weak excimers but the possibility of some monomer emission cannot be excluded.

Introduction

At the present time carbazole polymers are the subject of considerable interest. Poly(*N*-vinylcarbazole) (PVK) is well-known for its photoelectric properties[1,2] and its extremely effective excimer formation.[3-5] With the potential technological applications of polymeric substances exhibiting photoelectric properties, it is natural that the photophysics of these materials should be the object of considerable investigation. Many other types of carbazole polymers have been synthesized and studied with a view to elucidating the photophysics of excimer formation in carbazole polymers.

We report here a study of excimer formation in poly[N^{ϵ}-(9-carbazolyl)carbonyl-L-lysine] (PKL) (Figure 1). The characterization of this polymer has been reported earlier.[6] It has an α-helix conformation in solution and is of high molecular weight. The stereoregularity of the helix backbone may be expected to radically influence excimer formation and contribute therefore to our understanding of this phenomenon in polymers. Furthermore, at sufficiently high concentrations a cholesteric liquid crystalline phase is formed. The introduction of long-range molecular order can be expected to enhance the photoelectrical properties of polymeric systems and there is evidence that this is so.[7,8] As a first step in an investigation of the photophysics and photoelectrical properties of this interesting polymer, and their interrelation, we have studied intramolecular excimer formation in dilute fluid solution.

Experimental Section

General. The synthesis of PKL has been described previously.[6] *N*-Isopropylcarbazole (NPK) was synthesized according to ref 9 by refluxing carbazole and sodium hydroxide in acetone with the dropwise addition of isopropyl bromide. The product was precipitated, washed with water, and recrystallized from petroleum ether. PVK was a commercial product (BASF Luvican M170) and was precipitated from THF into isopropyl alcohol three times. The structure of PKL is shown in Figure 1. Dioxane was Fluka UV spectroscopic grade. Solutions were degassed by bubbling with nitrogen directly in the cuvettes. One minute was sufficient to attain constant fluorescence quantum yield and bubbling was continued for a further 2 min. This degassing procedure was adequate considering the short lifetimes observed. During prolonged lifetime measurements the sample chamber was purged with nitrogen. All measurements are reported at 25 °C. Solution concentrations were such that maximum absorbance in the low-energy absorption band was approximately 0.15–0.20 (ca. 5×10^{-5} M).

Spectra. Absorption spectra were recorded on a Cary 219 spectrophotometer.

Emission spectra were recorded on an Aminco SPF-500 spectrofluorimeter in the corrected quantum mode. Relative quantum yields were estimated by measuring the area under the emission curves and correcting for lamp intensity variations with exciting wavelength and variations in absorbance at the exciting wavelength. These corrections were always small.

Fluorescence Polarization. The anisotropy of the emission from PVK and PLK was measured with a double-beam instrument based on the configuration of Weber.[10] However, amplified photosignals were fed to a ratio meter, and monochromators were used for selecting excitation and emission wavelengths. Polarization effects in the monochromators were corrected for by using the Solleillet symmetry relations[11] as described in ref 10 and 12.

Time-Resolved Fluorescence Studies. Fluorescence decays were measured by the single-photon-counting technique using an instrument described elsewhere.[13] Excitation was by a gated flash lamp (PRA 510B, MACOR lamp body)[14] filled with N_2 at 0.3 atm using a 1.1-mm spark gap. The lamp was operated at 25 kHz. The emission was observed by an RCA8850 photomultiplier at 2.1 kV. The excellent energy discrimination properties of this multiplier were used to provide discrimination against multiphoton events, allowing counting rates up to 10% of the lamp frequency.

However, in the present study the maximum counting rates attainable were considerably less. At least 10^4 counts were collected in the maximally populated channel of the fluorescence time profile. The maximum of the lamp profile contained several times this number. Excitation and emission wavelengths were selected by monochromators (Jobin-Yvon H10UV and H10VIS) using bandwidths of 16 and 8 nm for excitation and emission, respectively. The time profile of the exciting pulse and the emission profile were recorded together by repeatedly switching the light path between a scattering solution (Ludox) and the sample solution. The emission profiles were analyzed by convolution of experimental lamp and model functions with least-squares fitting[15] using a modified Levenberg–Marquardt algorithm.[16]

Goodness of fit of the model was judged from χ_ν^2 defined as

$$\chi_\nu^2 = \frac{1}{N-n} \sum_{i=1}^{N} (R_i)^2$$

where the weighted residuals R_i are given by $R_i = (F_i^o - F_i^c)/(F_i^c)^{1/2}$, N is the number of channels used in the fitting procedure, n is the number of estimated parameters, F_i^c is the calculated intensity in channel i, and F_i^o is the observed intensity in channel i (intensity expressed in photon counts). To check that the residuals were randomly distributed about the calculated profile the number of runs was investigated (by a run is meant a series of neighboring data points all having either positive or negative residuals). The deviation of the observed number of runs from the most probable value is denoted by Z, expressed in standard deviations.[17] To

0024-9297/84/2217-1751$01.50/0

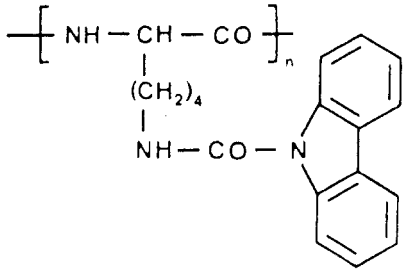

Figure 1. Chemical structure of poly[N^{ϵ}-(9-carbazolyl)-carbonyl-L-lysine] (PKL).

be acceptable, $|Z| < 2$ and ideally $Z \to 0$.

Error limits reported express the exactness with which the minimum in χ^2 is located with respect to variation in the given parameter. Reported amplitudes are normalized to give $\sum_i|\alpha_i| = 1$. Of necessity it is impossible to record the lamp and fluorescence profiles under identical conditions. Since the lamp profile varies with wavelength,[18] it must be recorded at the excitation wavelength whereas the fluorescence is recorded at a longer wavelength. This introduces a timing error since the transit time of the photomultiplier is a function of the wavelength of the photon impinging on the photocathode.[19] This effect can be approximated by a time shift of the observed lamp pulse relative to the fluorescence pulse before deconvolution while assuming that the anode pulse *shape* is independent of photon wavelength. In order to determine the time shift in a given experiment we can allow it to vary and seek that value giving the best fit as judged by χ^2. This has been found to work well for simple exponential decays but in the case of multiexponential decays, as reported in this work, the shift becomes a mere fitting parameter without physical significance and indeed a minimum in χ^2 may not be found with respect to variation in the shift. Therefore a calibration procedure was used to determine the shift as a function of photon wavelength.[20] For the photomultiplier used in this work it has been found that the shift can be expressed as[20] $s = k(\lambda_{em} - \lambda_{ex})$, with $k = -2.8 \times 10^{-3}$ ns·nm^{-1} in the λ range 300–560 nm.

Results and Discussion

Steady-State Measurements. Emission Spectra. Corrected quantum spectra of PKL, PVK, and NPK are reported together with their respective absorption spectra in Figure 2. The spectra are presented so that S_0–S_1 transitions are vertically in line to allow a visual comparison of the relative positions of the emissions. The S_0–S_1 absorption band of PKL is blue shifted into the S_0–S_2 band as compared with PVK and NPK but otherwise shows the same structure. NPK is included as a model showing the monomer emission of carbazole. This emission shows very well the expected mirror image relationship to the absorption spectrum and only a small Stokes shift. The emission of PVK is broad and almost structureless and is universally attributed to various excimer species.[3,4,21]

The emission from PKL is quite different. Whereas the PVK spectrum shows a slight shoulder at 420 nm, the PKL spectrum shows two well-resolved bands. The long-wavelength band corresponds closely to the shoulder of the PVK spectrum, which is attributed to a low-energy excimer,[3,4,21] but the PLK band shows a well-developed shoulder indicative of two overlapping bands. The short-wavelength band lies somewhat to the blue of the PVK peak and may be an unresolved doublet. Stokes shifts and relative quantum yields are given in Table I. The shift of the short-wavelength band of PKL is considerably greater than that of the monomer emission and the mirror image relationship to the absorption spectrum is absent. Excitation spectra were identical with absorption spectra and independent of emission wavelength. Change of solvent to the more polar dimethyl sulfoxide (Me_2SO) did not change the spectrum or the quantum

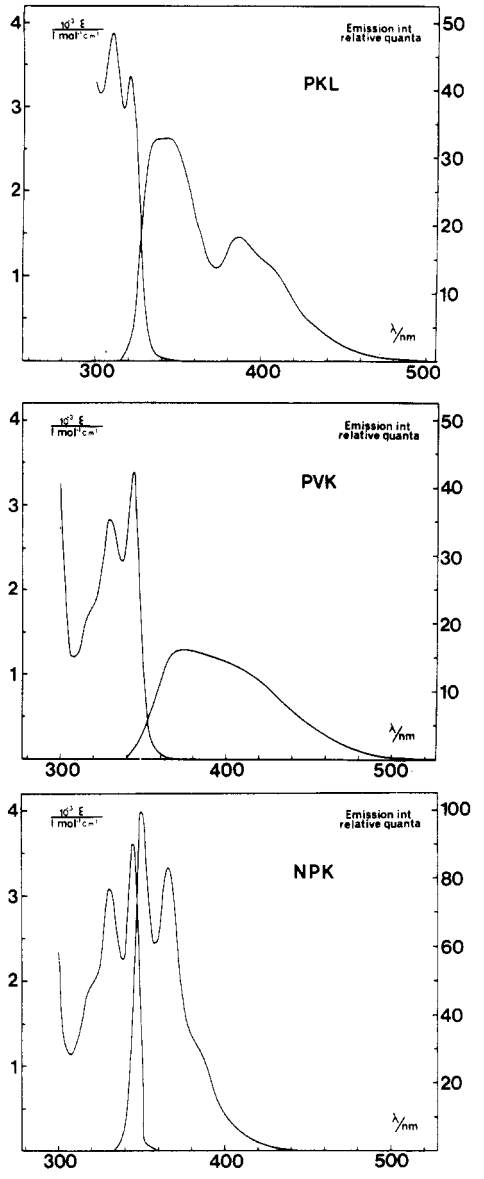

Figure 2. Absorption and quantum-corrected emission spectra of PKL (Figure 1), poly(vinylcarbazole) (PVK), and *N*-isopropylcarbazole (NPK) in N_2-saturated dioxane solutions. The S_0–S_1 absorption peaks are arranged to be vertically in line to allow a visual comparison of the Stokes shifts.

Table I
Stokes Shifts and Relative Quantum Yields for Some Carbazoles in N_2-Saturated Dioxane Solution

	Stokes shift, 10^6 m^{-1}	rel quantum yield
carbazole	0.052	0.94
isopropylcarbazole	0.042	1.00
PKL	0.16	0.69
PVK	0.22	0.42

yield, indicating the absence of exiplex formation between the carbazole and amide groups.

These results are strongly indicative of excited-state interactions which, however, may be weaker than in PVK since the carbazole groups are at the ends of flexible methylene chains, which allow greater variations in angles and distances between neighboring chromophores, leading to lower excimer binding energies. However, as discussed below, these weakly bound high-energy excimers can relax to low-energy excimer states via side-chain conformational changes, yielding the species emitting at longer wavelengths.

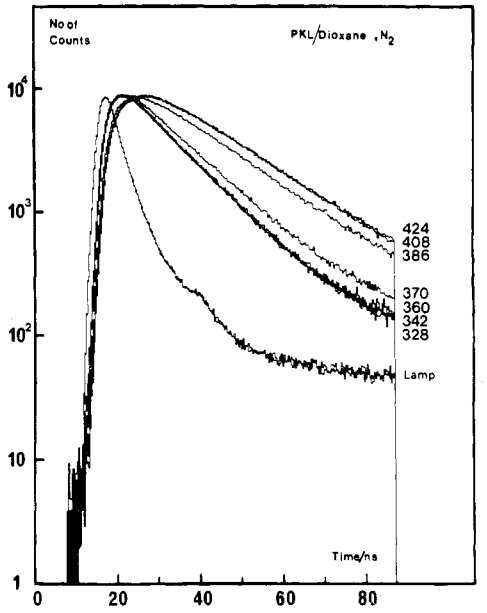

Figure 3. Fluorescence decays of PKL in N_2-saturated dioxane solution. A lamp profile was recorded together with each fluorescence decay (see text). The first and last lamp profiles of the series are shown, illustrating lamp stability. All curves normalized to 10^4 counts at peak. The emission wavelengths are given to the right.

Itaya et al.[22] report a single structureless emission band for poly[2-(*N*-carbazolyl)ethyl vinyl ether] (PKEVE) corresponding exactly to the high-energy band of PKL with the same Stokes shift (1990 and 1830 cm^{-1}, respectively). However, the long-wavelength band of PKL is totally absent in PKEVE. A significant difference between the polymers is the length of the methylene side-chain connecting the chromophore to the polymer backbone. The short chain in PKEVE may be too stiff to allow the formation of a low-energy carbazole sandwich excimer.

Studies on polymers of various isomeric vinylcarbazoles have shown that very little low-energy excimer is formed when bonding to the polymer backbone is at a ring carbon atom and high-energy excimers are not formed at all. This implies strict steric requirements for excimer formation in vinylcarbazole polymers, at least when the chromophore is attached directly to the polymer backbone. The degree of isotacticity in the chain is also of importance.[23,24] If the carbazole unit is attached via a more or less flexible methylene chain, the polymer conformation necessary for excimer formation will be more easily attained. However, the length of the chain may be critical.[25]

Polarization of the Emission. The degree of polarization of the emission of PKL was found to be zero at all wavelengths as observed for PVK.[26] Although the intrinsic polarization of the carbazole chromophore is low[31] ($p_0 \sim 0.1$), since the observed lifetimes are not unduly long and the chromophore is attached to a large stiff polymer molecule, we do not attribute the result to Brownian motion but rather to extensive migration between chromophores along the polymer chain.

Time-Resolved Studies. The decay of the emission from PKL was studied as a function of wavelength across the emission spectrum. The decay profiles are shown in Figure 3. A lamp profile was recorded simultaneously with each fluorescence decay but only the first and last in the series are shown in order to demonstrate lamp stability. The profiles group nicely into two sets corresponding to the two main well-resolved peaks in the emission spectrum at 342 and 390 nm, the curves at 370 and 386 nm being mixtures due to spectral overlap. Of the first group only

Scheme I

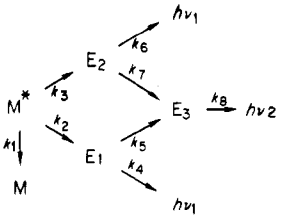

Scheme II

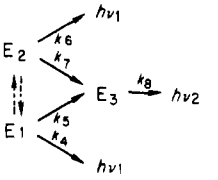

Scheme III

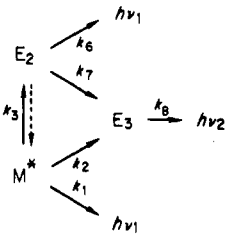

the emission at 342 nm was successfully analyzed, probably due to spectral overlap, whereas the emission at 386 nm gave the same results as at 408 nm. Results are reported in Table II. For multiexponential decays the percent contribution of each decay to the total observed emission is given.

A two-exponential analysis of the emission at 342 nm was possible but the shorter decay constant was significantly shortened by including early channels in the analysis, this indicating the presence of a third very short decay. Inclusion of a third decay improved the χ^2 and Z values. However, it is set in parentheses since its value varied from experiment to experiment (80–800 ps) and was dependent on the range over which the least-squares fit was performed. Our apparatus can determine subnanosecond single-exponential decays but certainly cannot be expected to more than indicate the presence of these in multiexponential decays. The fast decay represents only 1.6% of the total emission and may be due to monomer or simply be a fitting parameter. The emission at 342 nm arises from at least two species.

Analysis of the long-wavelength band demanded three exponentials, two of which had negative amplitudes corresponding to a buildup of this emission. In Table II both two- and three-exponential fits are included and clearly the triple exponential is a better representation of the data as judged from both χ^2 and Z. The rise times of the 408-nm emission correspond well with the decays of the 342-nm emission. The statistical uncertainty in the short time constant, 2.3 ± 0.5, should, however, be observed. This pattern in the time constants suggests that the species emitting at 408 nm arise from the species responsible for the 342-nm emission. If the two species emitting at 342 nm are both high-energy excimers, formed from the excited monomer via fast exciton migration to preformed sites along the polymer chain, analogous to PVK, the above results suggest kinetic Scheme I, which reduces to Scheme II if we assume k_2 and k_3 are very fast, thus explaining the lack of monomer emission. However, the short decay constant represents only 7% of the emission observed at

Table II
Decay Constants for the Emission of PKL in N_2-Saturated Dioxane Solution[a]

λ_{em}, nm	α_1, τ_1, ns	α_2 τ_2, ns	α_3 τ_3, ns	χ^2	Z
342	0.62 0.08 ± 0.2 (1.6%)	0.10 2.3 ± 0.5 (7.2%)	0.28 10.1 ± 0.1 (91%)	1.09	−0.43
408	−0.09 2.3 ± 0.5	−0.34 10.2 ± 0.2 −0.35 4.9 ± 0.3	0.57 14.6 ± 0.1 0.65 16.5 ± 0.2	0.966 1.34	0.84 −1.43
386	−0.09 2.6 ± 0.7	−0.30 10.7 ± 0.3	0.62 14.3 ± 0.1	1.15	0.13

[a] Excitation wavelength 310 nm. Bandwidths: ex = 16 nm, em = 8 nm.

342 nm and could be due to a monomer emission that in the steady-state spectrum is hidden under the broader excimer band of the second species. Scheme III may therefore be applicable. The differential equations for these schemes can be solved by using Laplace transforms and both yield for the time dependence of the emissions after δ-pulse excitation

$$f_{\nu_1}(t) = \alpha_1 e^{-yt} + \alpha_2 e^{-zt} \qquad \nu_1 = 342 \text{ nm}$$

$$f_{\nu_2}(t) = \alpha_3 e^{-wt} + \alpha_4 e^{-yt} + \alpha_5 e^{-zt} \qquad \nu_2 = 408 \text{ nm}$$

For scheme II, $y = k_4 + k_5$, $z = k_6 + k_7$, $w = k_8$, $\alpha_4 < 0$ if $w < y$, and $\alpha_5 < 0$ if $w < z$. Scheme III yields the same result except that $y = k_1 + k_2 + k_3$. This is in fact observed (Table II) with $y^{-1} = 2.3$ ns, $z^{-1} = 10.1$ ns. $w^{-1} = \alpha_5 = 14.6$ ns. It can be shown that $\sum_3^5 \alpha_i = 0$ but we observe $\sum_3^5 \alpha_i = 0.14$, noting that the amplitudes are normalized to $\sum|\alpha_i| = 1$. This is probably as good as can be expected.

The dotted arrows in Schemes II and III represent processes that are not observable since they represent interconversion between species observed at the same wavelength. Thus we should not expect to observe a separate term in $f_{\nu_1}(t)$ with a negative amplitude representing the buildup of E_1 from M* in Scheme III since this is included in α_1.

It is not possible to distinguish experimentally between Schemes I, II, and III at this point, and we shall include the possibility of two high-energy excimer states in our discussion. Temperature studies should help to resolve this problem.

The species emitting at 408 nm arise from those at 342 nm and we can therefore regard the 342-nm emission profile as the pumping function for the 408-nm emission just as the lamp profile is used as the pumping function for the 342-nm band.[27,28] If $F(t)$ is the observed decay and $f(t)$ is the true fluorescence decay function, while $L(t)$ is the excitation pulse, we have

$$\begin{aligned} F_{408}(t) &= L(t)*f_{408}(t) \\ &= L(t)*f_{342}(t)*f'_{408}(t) \\ &= F_{342}(t)*f'_{408}(t) \end{aligned}$$

where $f'_{408}(t)$ represents the *decay* of the 408-nm band, i.e., without buildup terms, and the asterisk denotes a convolution.

Thus, if $F_{408}(t)$ is recorded in the same experiment with $F_{342}(t)$ instead of $L(t)$, we can analyze for $f'_{408}(t)$. It should be noted that $f'_{408}(t)$ does not contain the terms $\alpha_4 e^{-yt}$ and $\alpha_5 e^{-zt}$ and we can therefore test for multiexponential *decay* in $f'_{408}(t)$. This is not possible in a direct analysis of $F_{408}(t)$ vs. $L(t)$ since we are in practice limited to three exponential terms. Furthermore, if due to spectral overlap the 408-nm emission includes a contribution from the 342-band, $\psi F_{342}(t)$, a constant term, ψ, is added to $f'_{408}(t)$ according to

$$\begin{aligned} F_{408}(t) = F_{342}(t)*f'_{408}(t) + \psi F_{342}(t) = \\ F_{342}(t)*[f'_{408}(t) + \psi] \end{aligned}$$

The results of this type of analysis are given in Table III.

Table III
Decay Constants for the Emission of PKL in N_2-Saturated Dioxane Solution at 408 nm[a]

α_1 τ_1, ns	α_2 τ_2, ns	α_3 τ_3, ns	χ^2	Z
A. Two-Exponential				
0.86 1.62 ± 0.5 (42%)	0.14 14.0 ± 0.3 (58%)		1.18	−0.16
B. Two Exponential Plus Constant[b]				
0.28 2.9 ± 0.3 (33%)	0.12 14.5 ± 0.2 (67%)	0.60	1.06	−1.00

[a] Deconvolution vs. the emission at 342 nm. Bandwidths: ex = 16 nm, em = 8 nm. [b] Allows for spectral overlap.

Scheme IV

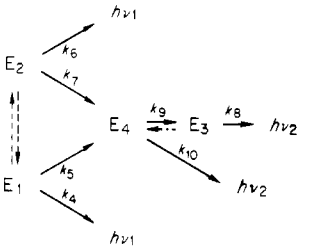

Scheme V

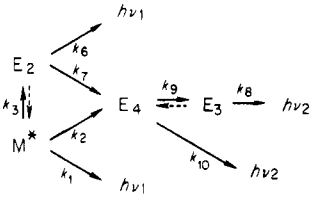

Scheme VI

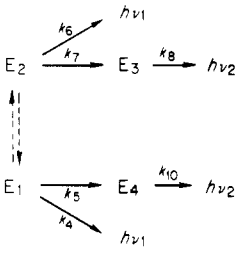

The species emitting at 408 nm arise from those at 342 nm and we can therefore regard the 342-nm emission profile as the pumping function for the 408-nm emission just as the lamp profile is used as the pumping function for the 342-nm band.[27,28] If $F(t)$ is the observed decay and $f(t)$ is the true fluorescence decay function, while $L(t)$ is the excitation pulse, we have

A single exponential could not fit the decays, a second shorter decay constant appearing together with the 14-ns decay already obtained by deconvolution of $F_{408}(t)$ with $L(t)$. Introducing a constant term improved χ^2 but gave a worse Z value. However, since the new τ changed significantly, we believe the constant term should be included. This second emission corresponds to 33% of the total at 408 nm.

If we can attribute this emission to a fourth species E_4, a second low-energy excimer, it can be incorporated into Schemes I–III in two ways in order to explain the observed decays. E_4 may be formed from E_1 (or M*) and E_2 as a precursor to E_3. Alternatively, E_3 and E_4 may be formed independently from E_2 and E_1 (or M*), respectively. The resulting possibilities are shown in Schemes IV–VII. From Table III we see that according to Schemes IV and V (k_9

Scheme VII

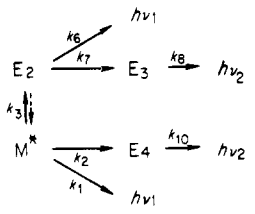

$+ k_{10})^{-1} = 2.9$ ns while according to Schemes VI and VII $k_{10}^{-1} = 2.9$ ns. $k_8^{-1} = 14.5$ ns in both cases.

Since E_4 and E_3 are observed at the same emission wavelength, in Schemes IV and V the decay of E_4 and the buildup of E_3 will give rise to only one exponential term with $\tau = (k_9 + k_{10})^{-1}$. Its amplitude and its sign will depend on the values of k_8, k_9, and k_{10}. For the same reasons a back-reaction from $E_3 \rightarrow E_4$ will not be observable. The inclusion of back-reactions would of course change the significance of the observed decay constants.

In all, four excited species appear to be involved in the emission from PKL. The species E_1 and E_2 could be preformed traps where the excited-state interactions are relatively weak due to the distance between and relative orientations of the carbazole chromophores involved. In PKL these chromophores are pendant to the α-helix via a four-carbon methylene chain which provides greater conformational mobility of nearest and next-nearest neighbors than in the case of PVK. That the excited-state interaction is less for the high-energy excimers in PKL than in PVK is also suggested by the lower Stokes shift (Table I) in PKL and would partly explain the better spectral resolution between high- and low-energy excimers observed in PKL. This is also probably the reason whey it is not necessary to invoke back-reactions from E_3 in Schemes I–III. Various types of nearest-neighbor pairs are possible but their number is limited due to the regular helix structure of the polymer. It appears that within the resolution of our technique we identify two species in the unresolved 342-nm emission band, one or both of which can be attributed to preformed excimer species. These represent two conformers or groups of conformers out of the total equilibrium distribution, having the appropriate distance and angular relationships between carbazole chromophores. Due to conformational differences these would be expected to relax with different rates to the lower energy more stable excimer states via side-chain conformational changes as is indeed observed. The ground-state conformation is known to affect the rate of intramolecular excimer and exciplex formation in simple molecules.[29,30]

Two low-energy excimer states appear to emit within the long-wavelength band, contrary to the accepted situation in PVK,[3-5] where a single low-energy fully overlapping sandwich dimer is proposed as the emitting species. The presence of a second lower energy excimer is in fact indicated by the long-wavelength shoulder of the second excimer band observed for PKK. That this is observed in PKL and not PVK may be due to the sterically pure structure of the polymer backbone in PKL.

We can only speculate on the difference between E_3 and E_4. Thus two carbazoles may lie coplanar but with their z axes not quite parallel or complete coplanarity may not be immediately attainable on steric grounds so that E_4 is first formed followed by further conformational relaxation to the fully overlapping sandwich dimer E_3, according to Schemes IV and V. Alternatively, according to Schemes VI and VII, we observe the independent relaxation of two distinct high-energy species to their respective low-energy excimers. The difference in E_3 and E_4 can then be attributed to the consequence of side-chain conformation and its relation to the position of the monomer in the helix structure.

Conclusion

The regular helical structure of PKL results in a much better resolution in the emission spectrum as compared with PVK and four excited species can be detected by the time-resolved technique. Two of these species are low-energy excimers formed from two high-energy excimeric species.

The present study does not allow us to decide which of the alternative schemes presented above is operative in PKL. It is hoped that a study of the low-temperature behavior of PKL and a more detailed study of the wavelength dependence of emission decay will help in further elucidating the photophysics of excimer formation in PLK and polycarbazoles in general. We must also bear in mind that in PKL the chromophore is connected via an amido linkage. We hope to synthesize a model to investigate possible effects of this.

The photophysics of PKL in its liquid crystalline phase is also of great interest in connection with its potential photoelectrical properties and their use in light energy transduction.

Acknowledgment. We thank Dr. J.-E. Löfroth for the use of his computer programs and generous advice on their use and Dr. Dorte Krabbe Munck for the NPK sample. D.B. acknowledges the financial support of the Swedish Natural Science Research Council. L.L.C. acknowledges financial support from Statens Tekniske Videnskabelige ForskningsrÅd and the B.P. Energifond.

Registry No. Poly[N^{ϵ}-(9-carbazolyl)carbonyl-L-lysine], 84110-21-4; PKL, 84117-59-9.

References and Notes

(1) H. Hoegl, *J. Phys. Chem.*, **69**, 755 (1965).
(2) P. J. Reucroft, K. Takahashi, and H. Ullal, *J. Appl. Phys.*, **46**, 5218 (1975).
(3) A. J. Roberts, D. Phillips, F. A. M. Abdul-Rasoul, and A. Ledwith, *J. Chem. Soc., Faraday Trans. 1*, **77**, 2725 (1981).
(4) G. E. Johnson, *J. Chem. Phys.*, **62**, 4697 (1975).
(5) D. Ng and J. E. Guillet, *Macromolecules*, **14**, 405 (1981).
(6) L. L. Chapoy, D. Biddle, J. Halstøm, K. Kovâcs, K. Brunfeldt, M. A. Qasim, and T. Christensen, *Macromolecules*, **16**, 181 (1983).
(7) Y. Park, M. A. Druy, C. K. Chiang, A. G. MacDiarmid, A. J. Heeger, H. Shirakawa, and S. Ikeda, *J. Polym. Sci., Polym. Lett. Ed.*, **17**, 195 (1979).
(8) L. W. Shacklette, H. Eckhardt, R. R. Chance, G. G. Miller, D. M. Ivory, and R. H. Baughman, in "Conductive Polymers", R. B. Seymour, Ed., Plenum Press, New York, 1981, p 115 ff.
(9) D. J. Cram, G. S. Hammond, "Organic Chemistry", 2nd ed., McGraw-Hill, New York, 1964, p 225.
(10) G. Weber, *J. Opt. Soc. Am.*, **46**, 962 (1956).
(11) P. Solleillet, *Ann. Phys.*, **12**, 23 (1929).
(12) T. Azumi and S. P. McGlynn, *J. Chem. Phys.*, **37**, 2413 (1962).
(13) J.-E. Löfroth, S. Bergström, and D. Biddle, in preparation.
(14) R. L. Lyke and W. W. Ware, *Rev. Sci. Instrum.*, **48**, 321 (1977).
(15) A. E. W. Knight and B. Selinger, *Spectrochim. Acta, Part A* **27**, 1223 (1971).
(16) International Mathematical & Statistical Libraries Inc., Houston, TX, routine ZXSSQ.
(17) N. R. Draper and H. Smith "Applied Regression Analysis", Wiley, New York, 1966, pp 95–99.
(18) Ph. Wahl, J. C. Anchet, and B. Donzel, *Rev. Sci. Instrum.*, **45**, 28 (1974).
(19) C. Lewis, W. R. Ware, L. J. Doemeny, and T. L. Nemzek, *Rev. Sci. Instrum.*, **44**, 107 (1973).
(20) D. Biddle and J.-E. Löfroth, in preparation.
(21) C. E. Hoyle, T. L. Nemzek, A. Mar, and J. E. Guillet, *Macromolecules*, **11**, 429 (1978).
(22) A. Itaya, K. Okamoto, and S. Kasabayashi, *Bull. Chem. Soc. Jpn.*, **49**, 2032 (1976).
(23) M. Keyanpour-Rad, A. Ledwith, and G. E. Johnson, *Macromolecules*, **13**, 222 (1980).
(24) J. L. Houben, B. Natucci, R. Solaro, O. Colella, E. Chiellini,

and A. Ledwith, *Polymer*, **19**, 811 (1978).
(25) M. Keyanpour-Rad, A. Ledwith, A. Hallam, A. M. North, M. Breton, C. Hoyle, and J. E. Guillet, *Macromolecules*, 11, 1114 (1978).
(26) M. Yokayama, T. Tamamura, M. Atsumi, M. Yoshimura, Y. Shirota, and H. Mikawa, *Macromolecules*, 8, 101 (1975).
(27) M. Almgren, *Chem. Scr.*, 6, 171 (1974).
(28) M. Almgren and C. Ch. Svensson, *Chem. Scr.*, 9, 145 (1976).
(29) R. Todesco, J. Gelan, H. Martens, J. Put, and F. C. De Schryver, *J. Am. Chem. Soc.*, **103**, 7304 (1981).
(30) M. Van der Anweraer, A. Gilbert, and F. C. De Schryver, *J. Am. Chem. Soc.*, **102**, 4007 (1980).
(31) Dorte Krabbe Munck, Thesis, The Technical University of Denmark.

Fine-Branching Structure in High-Pressure, Low-Density Polyethylenes by 50.10-MHz ^{13}C NMR Analysis

Takao Usami* and Shigeru Takayama

Plastics Research Laboratory, Mitsubishi Petrochemical Co., Ltd., Tohocho-1, Yokkaichi, Mie Prefecture, 510 Japan. *Received April 25, 1983*

ABSTRACT: The fine-branching structures in high-pressure, low-density polyethylenes (HP-LDPEs) have been studied by 50.10-MHz ^{13}C NMR analysis. When the ^{13}C NMR spectra of some HP-LDPEs are compared with those of some model polymers, it becomes clear that almost all ethyl branches consist of 1,3-paired ethyl groups and ethyl branches attached to quaternary backbone carbons rather than isolated ethyl branches and that there is no appreciable amount of hexyl branches in HP-LDPEs. The formation mechanism of these branches is consistent with a back-biting mechanism. The relative concentrations for various branch types were as follows: methyl, 2–3%; ethyl, 31–37%; propyl, ~2%; butyl, 34–37%; pentyl, 11–13%; longer branches, 14–16%. The fact that the HP-LDPEs studied here have almost the same relative concentrations for various branch types regardless of their different total methyl contents suggests that HP-LDPEs polymerized under ordinary conditions may be expected to have almost the same branching structure. The demonstration of the nonexistence of hexyl branches has almost dispelled the doubt that the contribution of intermediate-length branches (hexyl, heptyl, octyl, etc.) to the resonance for C-3 (third carbon from the branch end) might cause significant error in the estimation of longer chain branches (LCBs) in HP-LDPE by ^{13}C NMR.

Recently, branching in low-density polyethylenes prepared by free radical polymerization at high pressure (HP-LDPE) has been investigated in detail by ^{13}C NMR.[1-8] Of these branches, short-chain branches (SCBs) are mainly related to morphology and solid-state properties while long-chain branches (LCBs) are related to viscoelastic properties. Consequently, branching fine structure is very important for discussion of HP-LDPE properties. With respect to SCBs, the complexity and variability were pointed out by Axelson et al.[7] and Nishioka et al.,[8] but there are still some ambiguities concerning the type of ethyl branches and the existence of hexyl branches.

One purpose of this work is to elucidate the SCB fine structure in a manner consistent with branch formation mechanisms. Concerning quantitative analysis, the distribution of the various kinds of branches has been demonstrated to change so much depending on polymerization conditions[4] that there may not exist a typical HP-LDPE. However, there have been very few studies to establish this point. The reason seems to be that it is difficult to satisfy the quantitative conditions for ^{13}C NMR measurements and still obtain a high S/N ratio spectrum giving accurate integral intensities of the very small peaks (for example, the peaks from ethyl branches). A second purpose is to make it clear whether or not a typical HP-LDPE exists from the results for some HP-LDPEs prepared under different conditions.

Considering LCBs, it has been pointed out[5] that they could be estimated by ^{13}C NMR using the C-3 (third carbon from the branch end) resonance at ca. 32.2 ppm and some related reports were published.[7,9,10] However, this method has not come into general use despite its directness. On the other hand, two indirect solution methods (GPC–$[\eta]$ and M_w–$[\eta]$ methods) are conventionally utilized. There seem to be several reasons for this situation.

Table I
Ethylene/1-Olefin Copolymers Studied in This Work

copolymer	CH_3/1000 C main-chain atoms[a]
ethylene/1-propene	10.0, 23.5
ethylene/1-butene	8.0, 14.0, 21.0, 33.5
ethylene/1-hexene	7.5, 14.9
ethylene/1-octene	12.0, 15.5

[a] The concentrations were determined by ^{13}C NMR.

(a) First, there is the possibility of the existence of intermediate-length branches (hexyl, heptyl, octyl, etc.); these branches might cause significant error in the estimation of LCBs by the C-3 resonance because LCBs cannot be distinguished from the intermediate-length branches in the C-3 resonance. Recently, Mattice et al.[11] reported that calculations using a rotational isomeric state model for the chain statistics predict that the concentrations of intermediate-length branches would not be negligibly small.

(b) Second, there are some problems in quantitative analysis by ^{13}C NMR when minute peaks are compared with a large main peak: the dynamic range of both the A/D converter and the computer, differences in the spin–lattice relaxation times (T_1), and the nuclear Overhauser effects (NOEs) for various carbons.

(c) Third, there is interference by low molecular weight impurities: low molecular weight impurities also contribute to the C-3 resonance. Therefore, small amounts of impurities cause intolerable error for the estimation of LCBs. As a result, LCB values obtained by ^{13}C NMR and solution methods are not necessarily in good agreement.

Among these, problems b and c could be settled through refinement in the associated hardware and software, choice of the optimum measurement conditions, and sample purification through fractionation. Therefore, as the third purpose, problem a was studied to establish a reliable

0024-9297/84/2217-1756$01.50/0